# How Does the Growth of 5G mmWave Deployment Affect the Accuracy of Numerical Weather Forecasting?

Behzad Golparvar\*, Shaghayegh Vosoughitabar<sup>†</sup>, David Bazzett\*, Joseph F. Brodie<sup>‡</sup>,
Chung-Tse Michael Wu<sup>†</sup>, Narayan B. Mandayam<sup>†</sup>, Ruo-Qian Wang\*

\* Department of Civil and Environmental Engineering, Rutgers University, New Brunswick, New Jersey, USA

† WINLAB, Department of ECE, Rutgers University, New Brunswick, New Jersey, USA

‡ AKRF, Inc., Maryland, USA

Email: {behzad.golparvar, sha.vosoughitabar, db1142, ctm.wu, rq.wang}@rutgers.edu jbrodie@akrf.com, narayan@winlab.rutgers.edu

Abstract—The allocation of the 5G mmWave spectrum in the 26 GHz range, known as 3GPP band n258, has raised wide concern among the remote sensing and weather forecast communities due to the adjacency of this band with a frequency band used by passive sensors in Earth Exploration-Satellite Service (EESS). The concern stems from the potential radio frequency interference (RFI) caused by transmissions in the n258 band into the 23.8 GHz frequency, one of the key frequencies employed by weather satellite passive sensing instruments, such as AMSU-A and ATMS, to measure atmospheric water vapor using its emission spectrum. Such RFI can bias satellite observations and compromise weather forecasting. In this paper, we develop a modeling and numerical framework to evaluate the potential effect of the 5G mmWave n258 band's commercial deployment on numerical weather forecast accuracy. We first estimate and map the spatio-temporal distribution of 5G mmWave base stations at the county-level throughout the contiguous United States (US) using a model for technology adoption prediction. Then, the interference power received by the AMSU-A radiometer is estimated for a single base station based on models for signal transmission, out-of-band radiation, and radio propagation. Then, the aggregate interference power for each satellite observation footprint is calculated. Using the contaminated microwave observations. a series of simulations using a numerical weather prediction (NWP) model are conducted to study the impact of 5G-induced contamination on weather forecasting accuracy. For example, our results show that when the interference power at the radiometer from a single base station is at a level of -175 dBW for a network of base stations with spectral efficiency of 15 bit/s/Hz/BS, the aggregate interference power has limited impact in the year 2025 but can result in an induced noise in brightness temperature (contamination) of up to 17 K in the year 2040. Furthermore, that level of RFI can significantly impact the 12-hour forecast of a severe weather event such as the Super Tuesday Tornado Outbreak with forecasting errors of up to 10 mm in precipitation or a mean absolute error of 12.5%. It is also estimated that when the level of interference power received by the radiometer from a single base station is -200 dBW, then there is no impact on forecasting errors even in 2040.

Index Terms—Radio Frequency Interference (RFI), 5G mmWave, n258 band, Passive Sensors, AMSU-A, Numerical Weather Prediction (NWP)

This work was supported by the National Science Foundation (NSF) SWIFT program under Award No. 2128077. We acknowledge the Office of Advanced Research Computing (OARC) at Rutgers for the provided computing resources.

### I. Introduction

The sub-6 GHz frequency bands, traditionally employed for cellular communications, are facing increased demands due to the proliferation of connected devices and services. To accommodate these demands, 5G communication standards have adopted the inclusion of mmWave frequency bands, which present a potential avenue for enhanced spectrum availability [1]. Among the 5G mmWave bands are the 26 GHz (n258 band), 28 GHz (n257 band), 39 GHz (n260 band), and 47 GHz [2]. A noteworthy consideration is the proximity of the 3GPP band n258 to the 23.8 GHz frequency. This latter frequency is significant for meteorological instruments, such as the Advanced Microwave Sounding Unit (AMSU)-A [3] and the Advanced Technology Microwave Sounder (ATMS). The ATMS is the state-of-the-art microwave sensing instrument with functionality equivalent to AMSU and with improved sampling and coverage [4]. Installed on weather monitoring satellites, these sensors are tailored to assess atmospheric radiance, which is pivotal for estimating water vapor density in the atmosphere, with water vapor being a determinant factor in numerical weather prediction (NWP) models. Because 23.8 GHz is an ideal frequency band for water vapor the water molecules in the atmosphere have a resonance frequency of 22.235 GHz, and a frequency near this resonance is specifically suitable for water vapor measurement by passive spaceborne sensors [5]. In addition, water vapor has the highest electromagnetic signal absorption in this band compared to other bands, and this band is less sensitive to other atmospheric gases such as oxygen  $(O_2)$ , ozone  $(O_3)$ , carbon monoxide (CO), and nitrogen oxides (NO<sub>x</sub>) because these gases have different resonances. The sensitivity of the radiance measurement in terms of brightness temperature to geophysical parameters can be seen in Fig. 1.

The adjacency of the 23.8 GHz frequency to the 5G n258 band brings forth potential challenges in terms of radio frequency interference (RFI). There are some concerns in weather forecasting and earth remote sensing communities, including the National Oceanic and Atmospheric Administra-

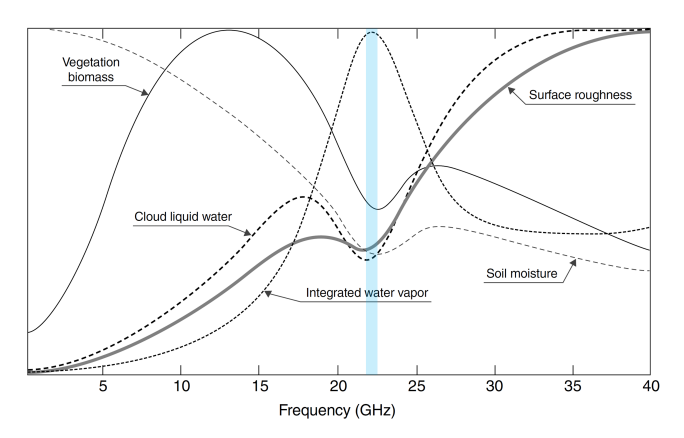


Fig. 1: Relative sensitivity of the microwave radiance measurement to geophysical parameters with frequency [5].

tion (NOAA), that there may be negative impacts on weather forecast accuracy due to the spectrum coexistence and RFI [6]–[8]. In fact, any unintended overlap between these bands could influence the measurements taken by the passive sensors on weather satellites. The potential energy leakage from the 5G bands into the 23.8 GHz spectrum might introduce variations in the measured atmospheric thermal emissions. Such deviations can introduce uncertainties in weather prediction models. Recent updates to the 3GPP's 5G NR technical specifications have been formulated with measures intended to protect meteorological satellite services. These measures advocate for reducing radiative emissions from adjacent 5G signals within the frequency range of 24.25 to 27.5 GHz [9]. However, NOAA asserts that the current emission standards fall short. They warn that without stricter control on 5G radiative emissions, the quality of vital data, crucial for accurate meteorological predictions, may be at risk. Therefore, there is a need to characterize and quantify the influence of 5G transmissions on weather data collection and subsequent prediction models.

There are limited studies in the literature that quantitatively assessed the impact of RFI in 23.8 GHz frequency on weather forecast accuracy. NOAA officials presented their estimation before the House Committee on Science, Space, and Technology that the -20 dBW/200 MHz limit first proposed by the Federal Communications Commission (FCC) as the out-ofband RFI threshold limit for 5G base stations is not sufficient because it would lead to a loss of passive microwave data by roughly 77 percent. It was also estimated that the microwave observation loss can degrade the forecast accuracy by 30% and in extreme conditions it can lead to a reduction in forecast lead time by 2 to 3 days for a hurricane track [10], [11]. In a study conducted by the European Centre for Medium-Range Weather Forecasts (ECMWF), it was determined through a modeling experiment that if all observations provided by polarorbiting satellites were unavailable, in a 5-day forecast, NWP models would not have provided any useful prediction that Hurricane Sandy would make devastating landfall on the New Jersey coast, and instead it was predicted that the hurricane would stay offshore in the Atlantic Ocean [12]. Although this study indicated the importance of satellite observations, it cannot specifically present a clear understanding of the impact of RFI in 23.8 GHz because all infrared and microwave sounding and imagers data were withheld in that study. In a study conducted by Palade et al. [13], aggregate uplink and downlink interference in the 23.8 GHz band were estimated for a network of interferers in New York City by considering realistic 3D building data and simulating ray-tracing propagation. Their results showed the level of aggregate RFI at the passive microwave sensor of AMSU-A onboard operational weather satellite MetOp-B from a high-density network of interferers is harmful under different levels of atmospheric attenuation, demonstrating that the concern raised by weather and remote sensing communities is well-founded.

To address this concern, there is a need to evaluate the impact of aggregate RFI caused by the spectrum coexistence on the accuracy and performance of data assimilation and to characterize the impact on weather forecast accuracy. In the previous study conducted by our team [14], the effect of 5G mmWave RFI in the 23.8 GHz band on the data assimilation-based weather forecast precision was investigated by considering uniform RFI throughout the contiguous United States assuming two 5G power leakage levels of -15 and -20 dBW, which was the least conservative leakage limits proposed by the FCC [11]. It was shown that the corresponding uniform induced noise in brightness temperature (contamination) was about 0.9 and 0.3 K, respectively, which could result in erroneous predictions of weather parameters. Since a few simplifying assumptions including geo-spatially uniform leaked power without RFI aggregation were used in that study, a more comprehensive study was needed to model different aspects of the problem in a relatively more realistic way. Following the previous preliminary studies [15], [16], a comprehensive investigation is conducted in this paper to evaluate the impact of 5G mmWave out-of-band RFI on the weather forecast accuracy by predicting the spatio-temporal distribution of 5G base stations throughout the US and considering a range of leaked power to understand what levels of leaked powers at passive sensors can be harmful to the NWP models. The predicted non-uniform distribution of 5G base stations is then used to calculate the aggregated leaked power for AMSU-A observations throughout the US. Then, by applying the aggregated induced noise (contamination) to radiance observational data in terms of brightness temperature, the impact of RFI is studied by conducting a series of weather forecast simulations using the Weather Research and Forecasting (WRF) NWP model to simulate weather processes along with WRF Data Assimilation (WRFDA) to process the radiance observational data. WRFDA and WRF are widely used in research and operational forecasting [17], [18].

# II. METHODOLOGY

# A. Spatio-Temporal Distribution of 5G Base Stations

The spatio-temporal estimation of the 5G mmWave deployment is complex and depends on several factors including

technical, financial, regulatory and other considerations such as zoning laws. As the focus of this paper is to assess the impact of the technology on weather forecast accuracy, the detailed spatial configuration of 5G mmWave transmitters is beyond the scope of this study. Therefore, the problem is simplified to estimate how this technology is adopted and diffused among users from its deployment start date to the later stages when its deployment becomes saturated. As 5G mmWave has significantly improved features such as higher speed and lower latency, the temporal trend of 5G mmWave n258 band adoption can be assumed to be somewhat similar to the growth patterns of broadband adoption [19], [20] since they both represent networks that have significantly advanced capabilities in comparison with their predecessors. The diffusion of a new technology in time typically has three main phases, including the early adoption stage, which has a very slow increase rate; the second phase with rapid increase in adoption rate; and the final phase, in which adoption of the technology becomes saturated, leading to tailing off the growth rate. This temporal evolution looks like an "S" shape, as shown in Fig. 2 for the broadband adoption depicted by blue markers during the time of its deployment on the upper x-axis. To apply this pattern to estimate the 5G mmWave deployment growth, the Gompertz diffusion model [21] is adopted to be trained on the broadband adoption data [22] using the nonlinear least squares (NLS) technique. The mathematical form of the model is expressed in Eq. 1,

$$Y_t = b_1 \exp(-b_2 \exp(-b_3 t)),$$
 (1)

where  $Y_t$  is the subscription percentage, t is time in year, and  $b_{1-3}$  are learnable parameters. Then, using the trained Gompertz model, 5G mmWave adoption is predicted in the number of subscribers in 100 population as shown in Fig. 2. Literature review revealed that the so-called 5G mmWave network rolled out in April 2019 for the first time in the US [23]; however, as frequency bands ranging from n257 to n261 are all classified as NR 5G mmWave frequency bands, it shouldn't be considered that the deployment in all of these bands would grow with equal rate. Furthermore, since the n258 is the frequency band of concern because of its potential impact on weather satellites, we only focus on predicting the deployment of 5G mmWave specific to the n258 band. According to [24], September 2021 is considered as the start date of the n258 band deployment in our modeling. We emphasize that while the exact growth pattern will shift if the deployment start date is earlier or later, the overall trends provided and the general conclusions drawn in the rest of the paper in regards to the impact of 5G mmWave deployment on weather forecasting are still valid.

Although 5G mmWave offers much faster data transfer speeds and lower latency than traditional cellular technologies, it also comes with some limitations, particularly in terms of coverage. Due to the high frequency of the mmWave spectrum, the signal cannot propagate far, making the technology more suitable and cost-effective for dense urban areas. Since the typical coverage radius of each mmWave base station is sig-

nificantly smaller than that of LTE sub-6 GHz, a large number of stations is required to have consistent and reliable coverage in suburban areas or small towns, which makes it unreasonable for network operators to justify the investment in 5G mmWave infrastructure in those less populated areas. Therefore, for the analyses presented in this paper, the mmWave network is only considered for dense urban areas, and the sub-6 GHz network is considered for such suburban and rural areas. Accordingly, using the county-level census data [25], only counties which are classified as metropolitan areas are taken into account to estimate the future adoption of 5G mmWave in terms of number of active subscribers, given that the percent of people

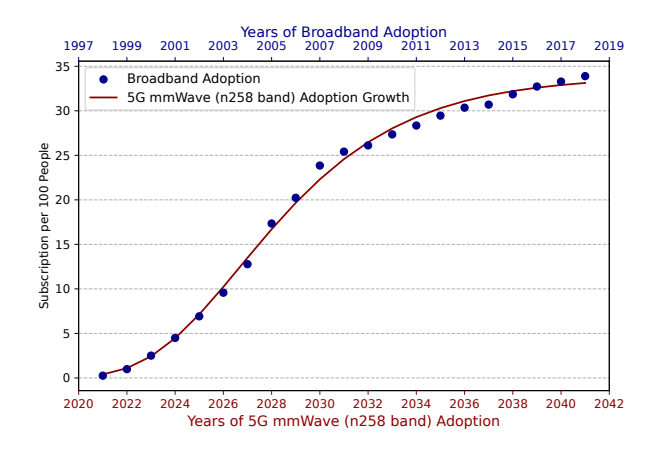


Fig. 2: 5G mmWave adoption growth rate predicted using Gompertz model [21].

subscribing to the technology and the population of the counties are known using the trained Gompertz model and census data, respectively. The total number of 5G mmWave base stations for each metropolitan county  $(N_c)$  can be estimated by  $N_c = D_t/(\eta_{sp} \times B)$  [19], where  $D_t$  is the total demand of a county, B is the bandwidth of 5G mmWave spectrum which can be as high as 500 MHz, and  $\eta_{sp}$  is spectral efficiency.  $D_t$ can be calculated by multiplying the number of subscribers by the average download speed demand per user of 100 Mbps, which is considered a minimum requirement for a high quality 5G mmWave network [26]. The spectral efficiency depends on several factors such as the specific implementation, the channel conditions, and the amount of bandwidth allocated to a particular transmission. In the literature, the spectral efficiency of 5G mmWave networks is reported in a wide range between 2 to 52 bit/s/Hz per base station (BS) [19], [26], [27], which can be attributed to the deployment condition and the number of antennas in a multiple-input multiple-output (MIMO) system. Here we adopted three values of 7, 15, and 25 bit/s/Hz/BS as the baseline spectral efficiency for different 5G deployment phases. It is evident that higher spectral efficiency results in a lower number of base stations and lower aggregate leakage. Considering the mentioned data processing and assumptions, the distribution of the base stations throughout the contiguous US is obtained for different deployment phases such as years 2025, 2030, and 2040. As an example, the distribution of 5G

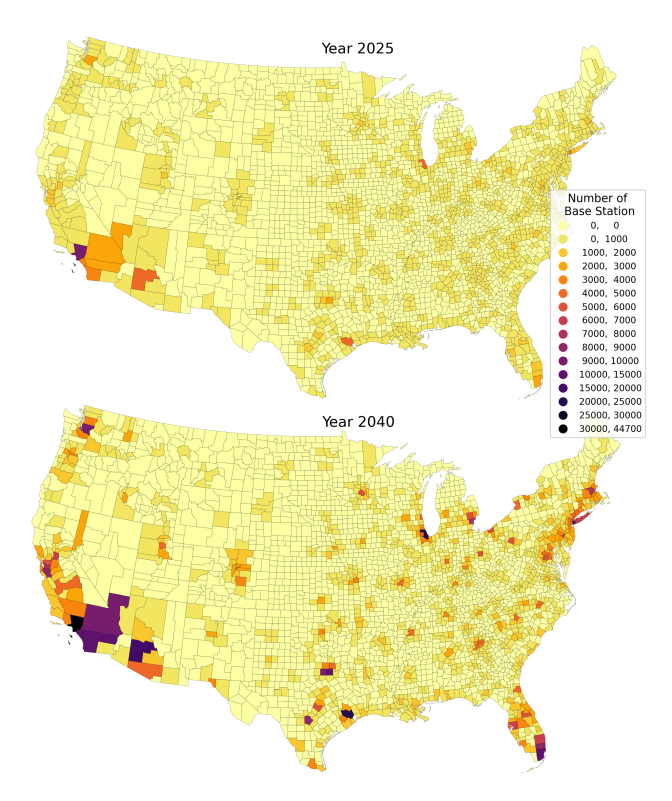


Fig. 3: Predicted number of base stations in each county for  $\eta_{sp}=15$  bit/s/Hz/BS in years 2025 and 2040

base stations with n258 transmitters is shown in Fig. 3 for spectral efficiency of 15 bit/s/Hz/BS and for the two years, 2025 and 2040. In the above, we emphasize that we have assumed that all base stations have the same spectral efficiency in every county. Further, the base station distributions within each county are assumed to be uniform because the data employed in the modeling is at the county-level resolution.

### B. Leakage from a Single Base Station

The filtering process is indispensable in the transmission of 5G signals. The critical role of filters lies in ensuring effective out-of-band suppression, preventing interference with other frequency bands used for purposes such as weather sensing. In this regard, for estimating the leaked power from the n258 band to the weather sensing band, we consider a scenario where a single base station transmits a signal in a channel ranging from 24.25 GHz to 24.75 GHz. This channel corresponds to the closest mm-wave 5G channel to the sensing band around 23.8 GHz. Taking into account two cases of weak and strong filtering, Fig. 4 illustrates the frequency responses of 2nd and 5th order Chebyshev filters with a bandwidth of 500 MHz and a center frequency of 24.5 GHz, with 0.2 dB ripple [28]. It is evident that the roll-off rate of a filter increases as its order rises, thereby the leakage to the weather sensing band around 23.8 GHz decreases by using a higher order filtering response in the base station side. One can obtain the power leakage from this channel to the weather sensing band through an integration over the AMSU-A sensing band, ranging from 23.665 GHz to 23.935 GHz, as follows [29]:

$$S_y(f) = S_x(f)|H(f)|^2, \quad S_x(f) = \frac{P}{BW},$$
 (2)

$$P_{\text{Leaked}} = \int_{23.665E9}^{23.935E9} S_y(f)df, \tag{3}$$

where H(f) represents the frequency response of the filter. Moreover,  $S_x(f)$  and  $S_y(f)$  indicate the power spectral densities of the input and output signals, respectively. P stands for the total power distributed over the transmission bandwidth of BW. Finally,  $P_{\text{Leaked}}$  indicates the leaked power to the weather sensing band, shown in Fig. 4.

Assuming P=10 W and BW=500 MHz,  $P_{\rm Leaked}$  is obtained to be -36 dBW and -44 dBW by having 2nd and 5th order filtering responses, respectively. Subsequently, by applying Friis formula in dB scale, the received interference power by the AMSU-A radiometer from a single base station  $(P_{\rm RFI}^S)$  is calculated as follows [28]:

$$P_{\text{RFI}}^{S} = P_{\text{Leaked}} + G_{\text{BS}} + G_{\text{AMSU-A}} - P_{L}, \tag{4}$$

$$P_L = 20\log\frac{4\pi R}{\lambda},\tag{5}$$

where  $G_{\rm BS}$  and  $G_{\rm AMSU-A}$  are the gains of the base station's antenna array and AMSU-A receiver, respectively. Additionally, R indicates the distance of the AMSU-A from Earth, and  $\lambda$  represents the wavelength of the leaked signal. Considering R=800 km, along with  $G_{\rm BS}=20$  dBi,  $G_{\rm AMSU-A}=34$  dBi representing their maximum values [13], [30] for the severe interference scenario where the main beam directions of the base station and the AMSU-A antenna patterns are assumed to be aligned toward each other. In this case, the highest leaked power reaching the satellite's receiver would be -160 dBW and -168 dBW with 2nd and 5th order filtering responses for the signal transmission, respectively. It is noted that if the 5G channel is far away from 23.8 GHz, the leakage would be negligible.

It is worth noting that the calculated values can vary depending on the transmitted power, orientations of the satellite's receiver and base station's transmitter, as well as the weather conditions, as investigated in [31]. Furthermore, as previously discussed, the type of filtering utilized in the base stations for transmitting 5G signals is another factor influencing the estimation of leaked power. In [31], the leaked power from a single base station — operating in the n258 band — is considered —3 dBm, which is the suggested limit for the protection of Earth exploration services [32]. The authors reported that this leaked signal from a single base station reaches the satellite with a power level between —330 dBW and —150 dBW, which is a considerably wide range due to the mentioned factors.

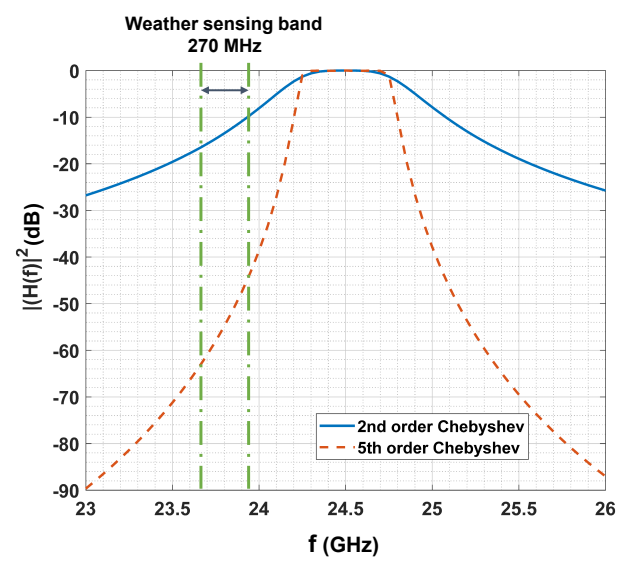


Fig. 4: Frequency responses of the 2nd and 5th order Chebyshev filters

# C. Calculation of Aggregate RFI

To calculate the aggregate RFI in terms of brightness temperature (contamination) a few processing steps are involved. First, it is necessary to locate weather satellite footprints and their corresponding observation coverage area to estimate the number of 5G base stations in each covered area, and subsequently to calculate the aggregate leaked power and induced noise in brightness temperature. In this study, the Super Tuesday Tornado Outbreak, which took place in the Southern United States and the lower Ohio Valley on February 5, 2008, is selected as a case study to investigate the 5G out-of-band RFI on the weather forecast precision. Therefore, all AMSU-A radiance observations covering the contiguous US are collected to be assimilated to update the initial and boundary conditions used for a 12-hour forecast simulation starting from 7 AM EST. The light blue circles shown in Fig. 5 are the AMSU-A observations from several satellites including Metop-A, NOAA-15, NOAA-16, and NOAA-18 measured approximately between 5 to 9 AM EST.

The AMSU-A instrument functions as a cross-track scanning radiometer, designed to observe radiance across 15 distinct channels. Within this array, 12 channels operate in the 50–60-GHz range, while the remaining 3 window channels are positioned at frequencies of 23.8, 31.4, and 89 GHz. The instrument operates by acquiring a sequence of 30 Earth observation scenesby employing a "stop and stare" methodology. It executes a scanning increment of 3.33 degrees, with a temporal resolution of 20 milliseconds for each sampling event. The instrument's antenna features a beam width characterized by a half-power beam width (HPBW) of 3.3 degrees, resulting in an Instantaneous Field of View (IFOV) approximately 48 km in diameter at nadir. The IFOV for larger scan angles is larger than that at nadir such that it reaches around 180 km, which results in the instrument resolution decreasing for the scan

positions near the limb region of the scan swath, as depicted in Fig. 5.

To calculate the aggregate RFI in terms of aggregate leaked power received by the AMSU-A radiometer, the distribution of base stations at the county level, and the leaked power at the radiometer from a single base station  $(P_{RFI}^S)$  are used. For each observation, the satellite footprint has a coverage area calculated using the satellite's zenith angle and its altitude. Each observation may cover parts of adjacent counties. Here, it is assumed that each observation is only affected by the leaked signals emitted from the base stations within the covered area of that observation, a reasonable assumption for mmWave propagation. Therefore, by calculating the percentage area from each nearby county covered by the observation we can obtain the coefficients of a weighted aggregation method (as shown in Fig. 5) to estimate the number of base stations in the covered area, and subsequently to calculate the total leaked power for that observation. This additional power results in higher brightness temperature measured by the AMSU-A instrument in its channel 1, which is the frequency of concern at 23.8 GHz. In the presence of leaked power, the total radio frequency power received by the sensor can be expressed using Eq. 6:

$$P_T = kT_B B + P_{\text{RFI}}^T, (6)$$

where B is the channel bandwidth in Hz,  $k=1.381 \times 10^{-23}$  J/K is the Boltzmann constant,  $T_B$  is the brightness temperature of the background radiation, and  $P_{\rm RFI}^T$  is the aggregate leaked power received by the radiometer obtained by  $P_{\rm RFI}^T = N_{\rm Obs}^{BS} \cdot P_{\rm RFI}^S$ , where  $N_{\rm Obs}^{BS}$  is the total number of base stations in the area covered by a single satellite observation, assuming that all  $N_{\rm Obs}^{BS}$  base stations operate at the same transmission power level. Accordingly, the induced noise in brightness temperature (contamination), which increases the scene brightness temperature, is obtained by  $\delta T = P_{\rm RFI}^T/kB$ . The  $\delta T$  represents the level of contamination in natural upwelling background radiation [33], and B is  $270 \times 10^6$  Hz. For the calculations in this step, we considered a wide range of  $P_{\rm RFI}^S$  to study the effects of received leaked power variations because it is a function of several varying

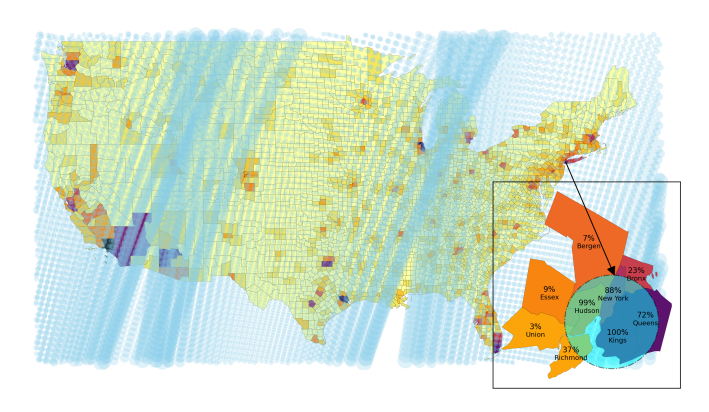


Fig. 5: AMSU-A observations from four satellites depicted as blue circles. Similar to Fig. 3(b) is in the background.

factors such as transmitter and receiver orientation, filtering response, atmospheric attenuation, etc. Using the aggregation method and the above-mentioned equation, the distribution of induced noise in brightness temperature (contamination) throughout the US is predicted for different  $P_{RFI}^{S}$  values and spectral efficiencies. For example, Fig. 6 shows the predicted distribution of the 5G induced noise in brightness temperature (contamination) for 5G mmWave (n258 band) deployment in years 2025 and 2040 for  $P_{\rm RFI}^S=-175$  dBW and spectral efficiency of 15 bit/s/Hz/BS. It can be seen that the highest levels of RFI are expected to happen in dense urban areas such as Chicago, New York City, and Los Angeles while most of the other counties have low levels of RFI. It should be noted that the maximum induced noise in brightness temperature can be as high as 18 K for this case in the year 2040, which is considerably high. Furthermore, such values could be even higher for higher received leaked power and lower spectral efficiencies.

# D. Data Assimilation-Based NWP model

NWP models incorporate data assimilation (DA) methodologies, utilizing real-time observational data acquired from various sensors and monitoring apparatus to refine and update their initial and boundary conditions, thereby diminishing forecast inaccuracies. Observational data of radiance, sourced from satellite measurements, constitute a critical category of inputs significantly influencing the NWP model's performance. These radiance observations are frequently integrated into variational DA algorithms employed by these models, with the aim of enhancing both the accuracy and reliability of meteorological predictions. In this study, WRFDA [17] is adopted as the data assimilation package and more specifically the 3D Variational DA algorithm (3DVAR) is used to assimilate the observations. Details of this algorithm can be found in [14], [34]. In WRFDA, the Community Radiative Transfer Model (CRTM) developed at the US Joint Center for Satellite Data Assimilation (JCSDA) is used as the radiative transfer model for processing the microwave observational data [35]. In the next section, numerical results of the weather forecast simulations are presented to analyze the potential impact of the 5G mmWave n258 frequency band on forecasts of the Super Tuesday tornado outbreak case [36].

# III. RESULTS AND DISCUSSION

# A. Weather Forecast Simulations

A series of forecast simulations with a 12-hour horizon were conducted for the extreme weather event of the Super Tuesday Tornado outbreak, focusing on a parametric analysis of various factors involved. These factors include leaked power received by the radiometer from a single base station  $(P_{\rm RFI}^S)$ , spectral efficiency  $(\eta_{sp})$ , and the timing of 5G mmWave deployment in year. To assess the deviation in forecasts, the parameter of accumulated total cumulus precipitation was chosen as a primary forecast parameter. This decision is informed by the fact that the concerned frequency, 23.8 GHz, corresponds to the

AMSU-A channel 1, which is predominantly utilized for observations of surface conditions and atmospheric precipitable water, while the majority of the other channels are dedicated to atmospheric temperature sounding [37]. Consequently, the most pronounced impact of RFI at this frequency is anticipated to be on the accuracy of weather forecasts pertaining to water vapor and precipitation parameters. It should be noted that other forecast parameters such as temperature, wind speed, cloud fraction, etc. are also affected by RFI, however, here we focus on precipitation forecast. Fig. 7(a) shows the distribution of the predicted accumulated total precipitation without any radio frequency interference. It can be seen that the maximum accumulated precipitation was around 37 mm. In Fig. 7(b), the impact of 5G mmWave n258 band with  $P_{\rm RFI}^S=-175$  dBW and spectral efficiency of 15 bit/s/Hz/BS in deployment year 2040 is presented in terms of deviation from forecast without RFI. It is shown that such a level of 5G mmWave RFI can affect the precipitation forecast up to 10 mm, which is a significant prediction error for a 12-hour forecast. It can also be seen that the forecast error is associated with regions where there was already predicted rainfall, and the RFI does not lead to an expanded area of forecasted precipitation. The impact of RFI on forecast results originates from the observation quality controls employed within the data assimilation process. There exist multiple quality controls and screening criteria that are interdependent across different channels. An overview of some

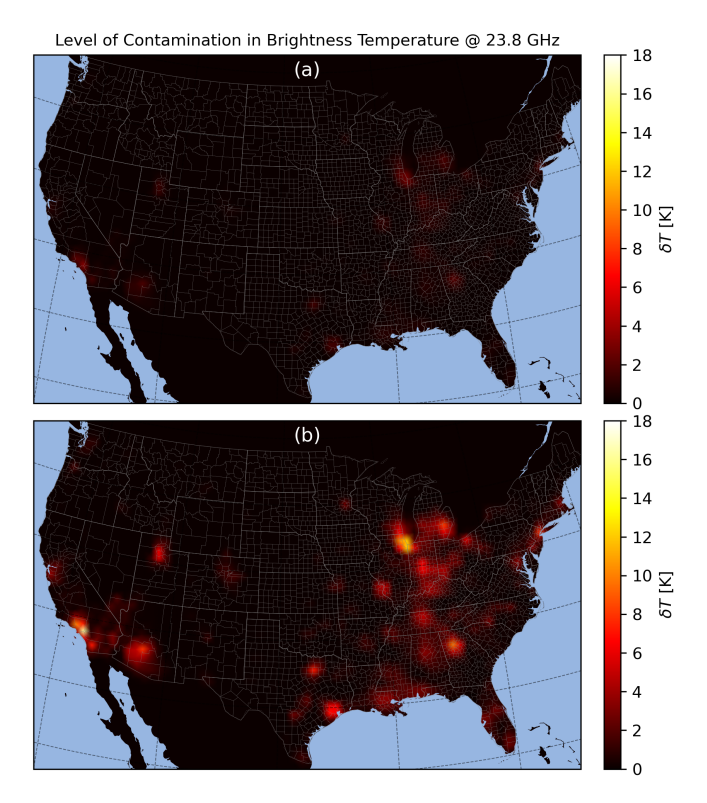


Fig. 6: Predicted RFI in terms of induced noise in brightness temperature (contamination) for  $P_{\rm RFI}^S=-175$  dBW and  $\eta_{sp}=15$  bit/s/Hz/BS in year (a) 2025, and (b) 2040

of the AMSU-A quality controls can be found in [38]. In essence, even though the brightness temperature data from AMSU-A channel 1 may not be used or assimilated directly for land surfaces, the contaminated data from this channel can still influence the quality flag of brightness temperature data in other channels. This, in turn, could lead to the loss of some observations in the presence of high levels of RFI. This can be attributed to the reason behind the distribution of forecast error shown in 7(b) where in some computational grids the error is negative and in some others the error is positive. The details of observations across different channels that are flagged as bad due to various RFI levels fall beyond the scope of this paper and will be considered in future work.

To see the impact of different RFI levels in terms of  $P_{\rm RFI}^S$ , spectral efficiency, and the deployment time of 5G mmWave n258 band, mean absolute percentage error (MAPE) is calculated for all cases. It should be noted that for this metric, the relative error was averaged only for the computational grids where the original precipitation value is non-zero. Fig. 8 shows the variations of MAPE versus interference power received by the radiometer from a single base station ( $P_{\rm RFI}^S$ ) for different spectral efficiencies in three deployment years. It can be seen that the spectral efficiency and deployment timeline determine the tolerable limit (0% MAPE) of 5G mmWave impact on precipitation forecast. For example, in the early stage of the deployment (year 2025), the permissible interference level

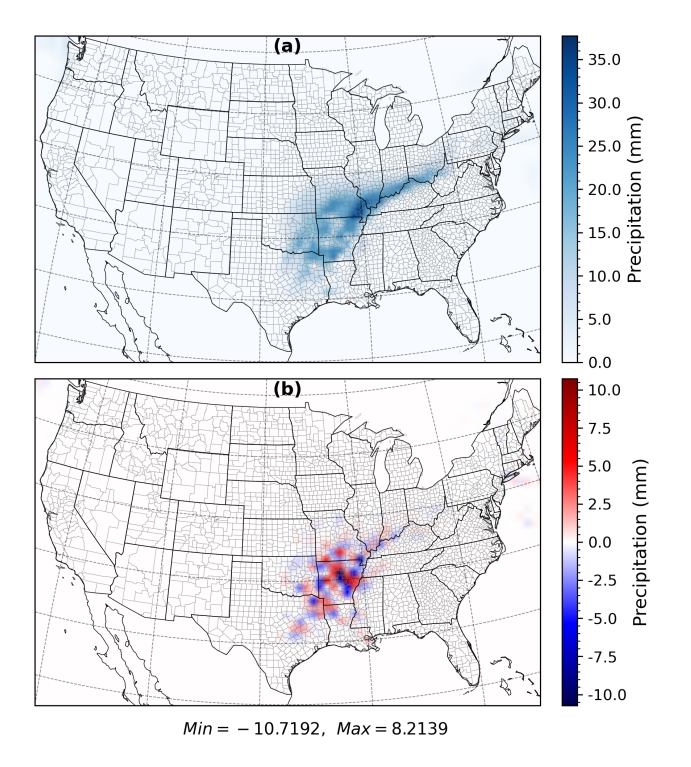


Fig. 7: (a) 12-hour forecast of accumulated total precipitation without any RFI, (b) deviation in accumulated total precipitation forecast for  $P_{\rm RFI}^S=-175$  dBW,  $\eta_{sp}=15$  bit/s/Hz/BS, and year 2040

received by the radiometer from a single base station can be as high as -195 dBW for spectral efficiencies of 15 and 25 bit/s/Hz/BS. However, this level will drop to -200 dBw in later deployment stages (2030 and 2040) with a higher number of base stations. It can also be seen that in the year 2040, if  $P_{\rm RFI}^S = -165$  dBW, the MAPE can be up to 20%, which is a significant level of potential error in the precipitation forecast.

## B. Perspective on Modeling and Results

We now discuss several aspects of the modeling and numerical results presented here. One consideration that should be taken into account is that not all 5G base stations are located outdoor. There should be also some picocells and microcells, which could be installed in indoor spaces such as shopping malls, large office buildings, etc.. When the base stations are located indoors, due to propagation losses there is almost surely no impact of any leakage on AMSU-A sensors. To investigate the effect of base station types in terms of installation environment (indoor vs. outdoor), it is required to estimate what percentage of total number of base stations are outdoor to estimate their impacts on weather satellite observations. As such, since the information about the future base stations is very limited, we undertake a parametric study by incorporating the outdoor base station percentage as a variable. As shown in Fig. 9, MAPE variations of accumulated total precipitation forecast is plotted versus  $P_{RFI}^{S}$  for different outdoor base station percentages. The graphs in this figure indicate that even if 70% of base stations are outdoor, the forecast errors due to the noise induced by outdoor 5G mmWave base stations are still significant and approximately the same as the case where all base stations are located outdoor. It is noteworthy that the trend of MAPE with an increase of interference power is generally increasing in both Figs. 8 and 9, however it may not be monotonic since there is a high degree of non-linearity in weather forecast algorithms that rely on data assimilation. In addition, under different RFI conditions, the geo-spatial distribution of dismissed observations changes in different ways because of the interdependency of channels in the quality control process within the DA algorithm [18].

Another consideration that should be noted is that the transmission power levels of base stations may not remain at full load throughout the day. Instead, to reduce energy consumption, the transmission power at each base station varies in accordance with the data traffic load. This variation is due to the fact that transmission power is adjusted based on the daily data traffic load profile, as a smaller number of user equipment (UE) are active during off-peak hours. On the other hand, AMSU-A instruments onboard different satellites provide microwave observations at different times, meaning that any possible impact on weather forecasts caused by 5G mmWave RFI is time-dependent. Cheng et al. [39] reported that the power level of macrocell and microcell base stations in an idle state can be as low as 55% and 75%, respectively, of the full load level during off-peak times. Accordingly, if we assume base stations operate at half full load power during off-peak time, it can be estimated that under this operating

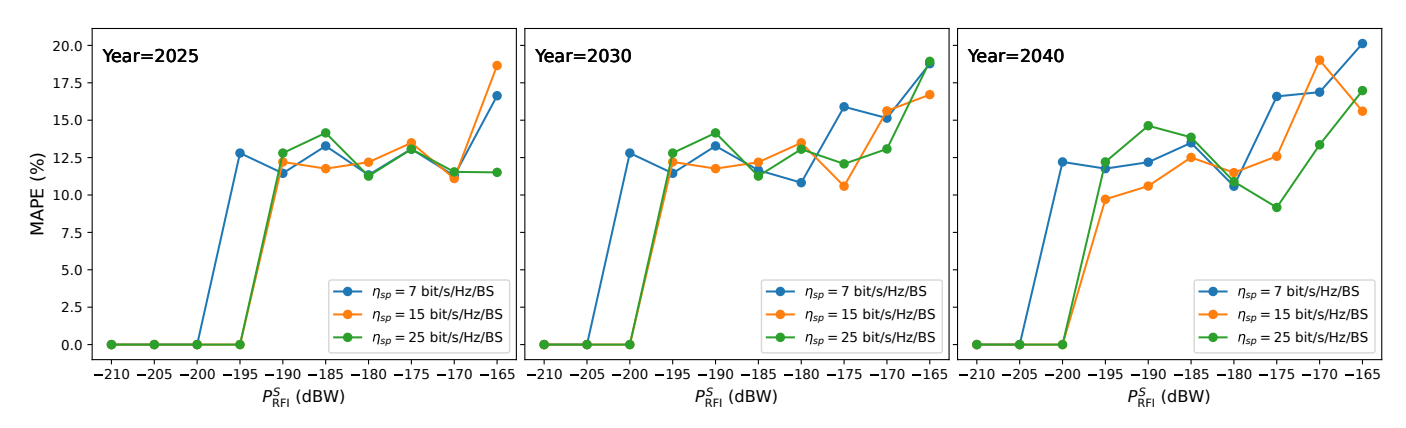


Fig. 8: Mean absolute percentage error of accumulated total precipitation forecast versus  $P_{\rm RFI}^S$  for different spectral efficiencies and deployment year

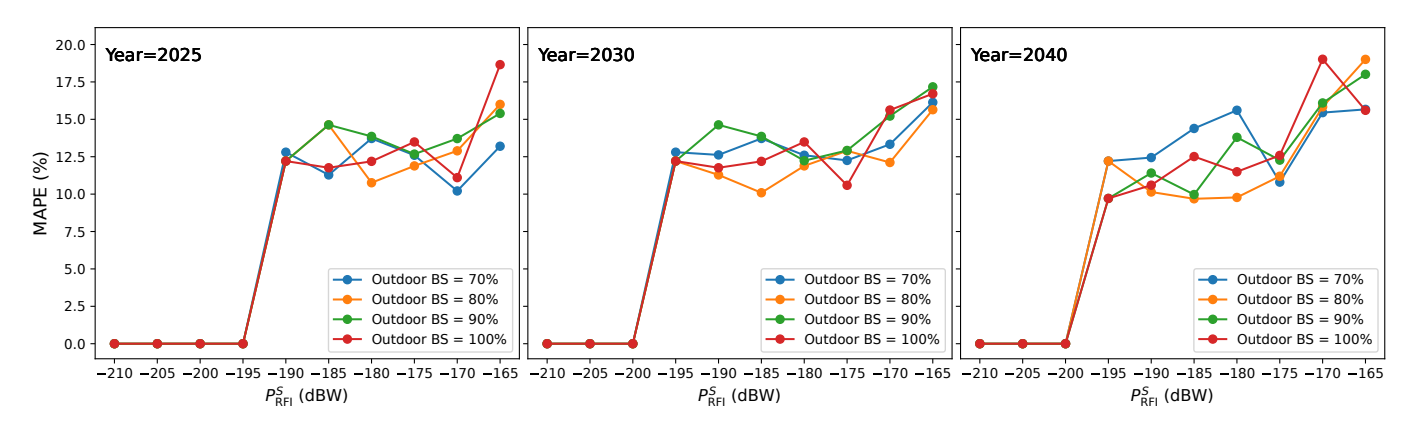


Fig. 9: Mean absolute percentage error of accumulated total precipitation forecast versus  $P_{\rm RFI}^S$  for  $\eta_{sp}=15$  bit/s/Hz/BS and different percentages of outdoor base stations, and three deployment times in year

condition the value of the leaked power at the radiometer from a single base station  $(P_{\rm RFI}^S)$  can be reduced by an order of -3 dBW. It should be noted that such level of variations in  $P_{\rm RFI}^S$  is already incorporated in our analyses. Specifically, we have conducted a parametric study on a wide range of  $P_{\rm RFI}^S$  from -210 dBW to -165 dBW, and it can be seen in Fig. 8 that around 3 dBW higher or lower interference power  $(P_{\rm RFI}^S)$  from some base stations can still lead to the same order of magnitude errors in weather forecasts.

In summary, while the exact 5G mmWave deployment growth pattern that emerges in practice is ongoing and yet to be determined, the overall trends provided and the numerical impact assessments in the paper on weather forecasting are still valid.

## IV. CONCLUSION AND FUTURE WORK

We developed a modeling and numerical framework to evaluate the potential effect of the 5G mmWave n258 band's commercial deployment on numerical weather forecast accuracy. By predicting the spatio-temporal distribution of 5G mmWave base stations at the US county level and considering signal transmission, out-of-band radiation, radio propagation and spectral efficiency, the aggregate interference power was

calculated for each AMSU-A satellite observation footprint to study the impact of contaminated microwave observations on weather forecasting accuracy. Results showed that if interference power at the radiometer from a single base station is at a level of -175 dBW for a network of base stations with a spectral efficiency of 15 bit/s/Hz/BS, the aggregate interference power has limited impact in the year 2025 but can result in an induced noise in brightness temperature (contamination) of up to 17 K in the year 2040. Furthermore, that level of RFI can significantly impact the 12-hour forecast of a severe weather event such as the Super Tuesday Tornado Outbreak with forecasting error of up to 10 mm in precipitation. The results also showed that if the level of interference power received by the radiometer from a single base station is -200 dBW, then there is no impact on forecasting errors even in 2040. The potential impact from the 5G mmWave n258 band on weather forecasting is increasingly relevant as deployment densities evolve, and needs renewed attention from both technological and policy perspectives. Future work will address the impact of 5G mmWave on weather forecasting using other NWP models such as the Unified Forecast System (UFS) [40].

### REFERENCES

- [1] T. S. Rappaport, S. Sun, R. Mayzus, H. Zhao, Y. Azar, K. Wang, G. N. Wong, J. K. Schulz, M. Samimi, and F. Gutierrez, "Millimeter wave mobile communications for 5g cellular: It will work!" *IEEE access*, vol. 1, pp. 335–349, 2013.
- [2] "5g millimeter wave frequencies and mobile networks," 2019.[Online]. Available: https://www.skyworksinc.com/-/media/SkyWorks/Documents/Articles/IWPC\_062019.pdf
- [3] Amsu-a. Accessed: 2023-10-25. [Online]. Available: https://space.oscar. wmo.int/instruments/view/amsu a
- [4] Atms. Accessed: 2023-10-25. [Online]. Available: https://shorturl.at/ekzP2
- [5] National Research Council, Handbook of Frequency Allocations and Spectrum Protection for Scientific Uses. Washington, DC: The National Academies Press, 2007, in English.
- [6] S. Hollister. 5g could mean less time to flee a deadly hurricane, heads of nasa and noaa warn. Accessed: 2019-05-01. [Online]. Available: https://shorturl.at/loqvW
- [7] S. Segan. No, 5g won't ruin your weather forecasts. Accessed: 2019-05-01. [Online]. Available: https://www.pcmag.com/opinions/ no-5g-wont-ruin-your-weather-forecasts
- [8] D. Kunkee and D. Lubar, "Passive microwave remote sensing and 5g: Key aspects of adjacent band operation in the mmw bands," in *Proceedings of the XYZ Conference*. 100th American Meteorological Society Annual Meeting, 2020. [Online]. Available: https://ams.confex.com/ams/2020Annual/meetingapp.cgi/Paper/371265
- [9] "5g nr user equipment (ue) radio transmission and reception; part2: Range 2 standalone," 3GPP, Tech. Rep. 38.101-2, 6 2019, 3GPPTechnical Specification. Version 15.3.0 Release 15.
- [10] US Congress. House. Committee on Science, Space & Technology, "The future of forecasting: Building a stronger u.s. weather enterprise: Hearing before the subcommittee on the environment," 116th Cong., 1st session., May 2019, https://www.govinfo.gov/app/details/ CHRG-116hhrg36302/summary.
- [11] S. E. Benish, G. H. Reid, A. Deshpande, S. Ravan, and R. Lamb, "The impact of emerging 5g technology on us weather prediction," *Journal* of Science Policy & Governance, vol. 17, no. 2, 2020.
- [12] T. McNally, M. Bonavita, and J.-N. Thépaut, "The role of satellite data in the forecasting of hurricane sandy," *Monthly Weather Review*, vol. 142, no. 2, pp. 634–646, 2014.
- [13] A. Palade, A. M. Voicu, P. Mähönen, and L. Simić, "Will emerging millimeter-wave cellular networks cause harmful interference to weather satellites?" *IEEE Transactions on Cognitive Communications and Net*working, pp. 1–1, 2023.
- [14] M. Yousefvand, C.-T. M. Wu, R.-Q. Wang, J. Brodie, and N. Mandayam, "Modeling the impact of 5G leakage on weather prediction," in 2020 IEEE 3rd 5G World Forum (5GWF), 2020, pp. 291–296.
- [15] B. Golparvar, I. B. Majumdar, S. Vosoughitabar, J. F. Brodie, N. Mandayam, C.-T. M. Wu, and R. Wang, "A study on the impact of non-uniform 5g leakage on the accuracy of weather forecasts," in AGU Fall Meeting Abstracts, vol. 2022, 2022, p. 5.
- [16] B. Golparvar, S. Vosoughitabar, I. B. Majumdar, J. F. Brodie, N. Mandayam, C.-T. M. Wu, and R.-Q. Wang, "Impact of future spatio-temporal 5g leakage on weather forecasting accuracy," in 103rd AMS Annual Meeting Poster presentation. AMS, 2023.
- [17] D. Barker, X.-Y. Huang, Z. Liu, T. Auligné, X. Zhang, S. Rugg, R. Ajjaji, A. Bourgeois, J. Bray, Y. Chen, M. Demirtas, Y.-R. Guo, T. Henderson, W. Huang, H.-C. Lin, J. Michalakes, S. Rizvi, and X. Zhang, "The weather research and forecasting model's community variational/ensemble data assimilation system: Wrfda," *Bulletin of the American Meteorological Society*, vol. 93, no. 6, pp. 831 843, 2012.
- [18] W. C. Skamarock, J. B. Klemp, J. Dudhia, D. O. Gill, D. Barker, M. G. Duda et al., "A description of the advanced research wrf version 3," University Corporation for Atmospheric Research, NCAR/TN-475+STR, 2008.
- [19] A. Jha and D. Saha, "Techno-economic analysis of 5g deployment scenarios involving massive mimo hetnets over mmwave: A case study on the us state of texas." 2018.
- [20] G. Intelligence, "Understanding 5g: Perspectives on future technological advancements in mobile," *White paper*, pp. 1–26, 2014.
  [21] N. Meade and T. Islam, "Technological forecasting—model selection,
- [21] N. Meade and T. Islam, "Technological forecasting—model selection, model stability, and combining models," *Management science*, vol. 44, no. 8, pp. 1115–1130, 1998.

- [22] I. T. U. (via World Bank), "Landline internet subscriptions per 100 people, 1998 to 2021," https://ourworldindata.org/grapher/broadband-penetration-by-country?tab=chart&facet=none&country=~USA, accessed: March 2023.
- [23] E. Oswald and C. de Looper, "Verizon 5G: Everything You Need to Know," https://www.digitaltrends.com/mobile/verizon-5g/, 2023, accessed: March 2023.
- [24] List of 5g nr networks: Commercial deployment. Accessed: 2023-11-08. [Online]. Available: https://en.wikipedia.org/wiki/List\_of\_5G\_NR\_ networks
- [25] USDA, Economic Research Service, "Data for 3142 counties in the united states," https://www.openintro.org/data/?data=county\_complete, 2023, accessed: March 2023.
- [26] F. Agnoletto, P. Castells, E. Kolta, and D. Nichiforov-Chuang, "The economics of mmwave 5g: An assessment of total cost of ownership in the period to 2025," GSMA Intelligence, 2020.
- [27] "5g millimeter wave frequencies and mobile networks: A technology whitepaper on key features and challenges," 2019. [Online]. Available: https://www.skyworksinc.com/-/media/SkyWorks/ Documents/Articles/IWPC\_062019.pdf
- [28] D. Pozar, Microwave Engineering. Wiley, 2011.
- [29] I. B. Majumdar, S. Vosoughitabar, C.-T. Michael Wu, N. B. Mandayam, J. F. Brodie, B. Golparvar, and R.-Q. Wang, "Resource allocation using filtennas in the presence of leakage," in 2022 IEEE Future Networks World Forum (FNWF), 2022, pp. 591–596.
- [30] ITU-R, "Typical technical and operational characteristics of earth exploration-satellite service (passive) systems using allocations between 1.4 and 275 ghz," https://www.itu.int/dms\_pubrec/itu-r/rec/rs/ R-REC-RS.1861-1-202112-I!!PDF-E.pdf, accessed: December 2021.
- [31] A. Palade, A. M. Voicu, P. Mähönen, and L. Simić, "Will emerging millimeter-wave cellular networks cause harmful interference to weather satellites?" *IEEE Transactions on Cognitive Communications and Net*working, pp. 1–1, 2023.
- [32] "NR; Base Station (BS) radio transmission and reception (3GPP TS 38.104 version 18.1.0 Release 18)," Mar 2023. [Online]. Available: https://www.3gpp.org/dynareport?code=38-series.htm
- [33] D. Kunkee, Radio-Frequency Interference (RFI) in Passive Microwave Sensing. New York, NY: Springer New York, 2014, pp. 634–639. [Online]. Available: https://doi.org/10.1007/978-0-387-36699-9\_153
- [34] Z. Liu, C. S. Schwartz, C. Snyder, and S.-Y. Ha, "Impact of assimilating amsu-a radiances on forecasts of 2008 atlantic tropical cyclones initialized with a limited-area ensemble kalman filter," *Monthly Weather Review*, vol. 140, no. 12, pp. 4017 4034, 2012.
- [35] Q. Liu, P. van Delst, Y. Chen, D. Groff, Y. Han, A. Collard, F. Weng, S.-A. Boukabara, and J. Derber, "Community radiative transfer model for radiance assimilation and applications," in 2012 IEEE International Geoscience and Remote Sensing Symposium, 2012, pp. 3700–3703.
- [36] J. L. Hayes, "Super Tuesday Tornado Outbreak of February 5-6, 2008," in Service Assessment, U.S. Department of Commerce, NOAA, March 2009
- [37] Z. Lai and S. Peng, "The effect of assimilating amsu-a radiance data from satellites and large-scale flows from gfs on improving tropical cyclone track forecast," *Atmosphere*, vol. 13, no. 12, p. 1988, 2022.
- [38] W. He, Z. Liu, and H. Chen, "Influence of surface temperature and emissivity on amsu-a assimilation over land," *Acta Meteorologica Sinica*, vol. 25, no. 5, pp. 545–557, 2011.
- [39] X. Cheng, Y. Hu, and L. Varga, "5g network deployment and the associated energy consumption in the uk: A complex systems' exploration," *Technological Forecasting and Social Change*, vol. 180, p. 121672, 2022. [Online]. Available: https://www.sciencedirect.com/ science/article/pii/S0040162522002049
- [40] "The unified forecast system (ufs)," https://ufscommunity.org/, accessed: November 2023.